Unusual biogenic calcite structures in two shallow lakes, James Ross Island, Antarctica

J. Elster[1,2]*, L. Nedbalová[2,3], R. Vodrážka[4], K. Láska[5], J. Haloda[4], J. Komárek[1,2]

[1] {Centre for Polar Ecology, Faculty of Science, University of South Bohemia, Na Zlaté Stoce 3, 37005 České Budějovice, Czech Republic}

[2] {Institute of Botany, Academy of Sciences of the Czech Republic, Dukelská 135, 37982 Třeboň, Czech Republic}

[3] {Faculty of Science, Charles University in Prague, Albertov 6, 12843 Prague, Czech Republic}

[4] {Czech Geological Survey, Klárov 3, 11821 Prague, Czech Republic}

[5] {Faculty of Science, Masaryk University in Brno, Kotlářská 2, 61137 Brno, Czech Republic}

Correspondence to: J. Elster (jelster@prf.jcu.cz)

Abstract

The floors of two shallow endorheic lakes, located on volcanic surfaces on James Ross Island, are covered with calcareous organosedimentary structures. Their biological and chemical composition, lake water characteristics, and seasonal variability of the thermal regime are introduced. The lakes are frozen down to the bottom eight-nine months per year and their water chemistry is characterized by low conductivity and neutral to slightly alkaline pH. The photosynthetic microbial mat is composed of filamentous cyanobacteria and microalgae that are considered to be Antarctic endemic species. The mucilaginous black biofilm is covered by green spots formed by a green microalga and the macroscopic structures are packed together with fine material. Thin sections consist of rock substrate, soft biofilm, calcite spicules and mineral grains originating from different sources. The morphology of the spicules is typical of calcium carbonate monocrystals having a layered structure and specific surface texture, which

reflect growth and degradation processes. The spicules chemical composition and structure correspond to pure calcite. Lakes age, altitude, morphometry, geomorphological and hydrological stability, including low sedimentation rates, together with thermal regime predispose the existence of this community. We hypothesize that the precipitation of calcite is connected with the photosynthetic activity of the green microalgae that were not recorded in any other lake in the region. This study has shown that the unique community producing biogenic calcite spicules is quite different to any yet described.

1 Introduction

The floors of most Antarctic lakes are covered with photosynthetic microbial mats (Vincent and Laybourn-Parry, 2008). However, the degree of disturbance plays a key role in the development of microbial mats. When growing in low-disturbance habitats, interactions between benthic microbial communities and their environments can produce complex emergent structures. Such structures are best developed in extreme environments, including benthic communities of deep, perennially ice-covered Antarctic lakes, where physical and chemical conditions, and/or geographical isolation preclude the development of larger organisms that could otherwise disrupt organised microbial structures (Wharton, 1994; Andersen et al., 2011). Many organosedimentary structures that emerge in these conditions are laminated and accrete through episodic trapping of sediments or grains and precipitation of minerals within a growing biogenic matrix (e.g. Arp et al., 2001; Reid et al., 2003). In perennially ice-covered lakes, the seasonality of growth imposed by the summer-winter light-dark conditions can induce annual growth laminations (Hawes et al., 2001), reinforced by calcite precipitation during growth and sediment diagenesis (Wharton et al., 1982; Wharton, 1994; Sutherland and Hawes, 2009). Calcite precipitation is not, however, a prerequisite for laminated, stromatolite-like communities (Walter, 1976; Schieber, 1999; Yamamoto et al., 2009). A diversity of micro- to nanostructured $CaCO_3$ associated with extracellular polymeric substances and prokaryotes was described from the sediments of an East Antarctic lake (Lepot et al, 2014). There is also a growing experimental evidence that some carbonate precipitates are only produced in the presence of organic matter (Cölfen and Antonietti, 1998; Pedley et al., 2000).

Precipitation of calcite by expulsion (segregation) is also a common process in the nature related to the freezing of common low ionic strength Ca^{2+} - HCO_3^- waters. Calcite precipitation related to water freezing was observed and described also from various polar-

alpine settings, e.g. from lake bottoms of Dry Valleys in Antarctica (Nakai et al., 1975) or as a results of aufeis (icing, naled) formation in Northern Canada (Clark and Lauriol, 1997). Crystalline precipitates that form subglacially on bedrock were reported from numerous locations (Ng and Hallet, 2002), for example fine-grained calcite powders were observed in subglacial deposits and in aufeis formations, Svalbard (Wadham et al., 2000) or in basal ice and subglacial clastic deposits of continental glaciers of Switzerland (Fairchild et al., 1993). Calcite pendants occurred beneath coarse clasts in well-drained sediments on Svalbard (Courty et al., 1994) and calcite coatings were found in cavities in cold-climate Pleistocene deposits of Western Transbaikalia, Russia, and in modern surface deposits at Seymour Island, Antarctica (Vogt and Corte, 1996).

James Ross Island belongs to a transitory zone between the maritime and continental Antarctic regions (Øvstedal and Lewis Smith, 2001). Air temperature records indicate progressive warming trends from 1.5 °C to 3.0 °C over the Antarctic Peninsula during the past 50 years (Turner et al., 2014). More than 80% of the island surface is covered with ice (Rabassa et al., 1982). Only the northernmost part of the island, the Ulu Peninsula, is significantly deglaciated and represents one of the largest ice-free areas in the northern part of the Antarctic Peninsula. The origin of the lakes on James Ross Island is related to the last glaciations of the Antarctic Peninsula ice sheet and retreat of the James Ross Island ice cap during the late Pleistocene and Holocene (Nývlt et al., 2011; Nedbalová et al., 2013). Interactions between volcanic landforms and glacial geomorphology during previous glacial-interglacial cycles, the Holocene paraglacial and periglacial processes and relative sea level change have resulted in the complex present-day landscape of James Ross Island (Davies et al., 2013). All of these processes have influenced the development of the lakes which are found on the Ulu Peninsula at altitudes from <20 m above sea level (a.s.l.) near the coast to 400 m a.s.l. in the mountain areas (Nedbalová et al., 2013).

During two Czech research expeditions (2008 and 2009) to James Ross Island, lake ecosystems of the Ulu Peninsula were studied in respect to their origin, morphometry, physical, chemical and biological characteristics (Nedbalová et al., 2013), together with detailed cyanobacterial and microalgal diversity descriptions (Komárek and Elster, 2008; Komárek et al., 2011; Kopalová et al., 2013; Škaloud et al., 2013; Komárek et al., 2015). As part of this study, we encountered 1 to 5 millimetres scale calcareous organosedimentary structures on the floor of two endorheic lakes, 1 and 2, which are quite different to any microbially mediated structures yet described from modern environments. These shallow

lakes on higher-lying levelled surfaces originated after the deglaciation of volcanic mesas which became ice-free some 6.5–8 ka ago (Johnson et al., 2011) and are considered among one of the oldest in the region. However, a later appearance of these lakes is also possible, as we have no exact dates from their sediments (Nedbalová et al., 2013).

The aim of this paper is to describe in detail the chemical and biological composition of the organosedimentary structures together with the limnological characteristics of the two lakes. A hypothesis concerning the formation of calcite spicules is also presented. The results of this study can serve as a baseline for understanding microbial behaviors in forming these organosedimentary structures, which will provide insight into the interpretation of fossil forms from early Earth.

2 Materials and methods

2.1 Study site

Endorheic lake 1 (63°54'11.7" S, 57°46'49.9" W, altitude 65 m a.s.l.) and endorheic lake 2 (63°53'54.6" S, 57°46'33.8" W, altitude 40 m a.s.l.) are shallow lakes located near Andreassen Point on the E coast of the deglaciated Ulu Peninsula, in the northern part of James Ross Island, NE Antarctic Peninsula (Figure 1). They are shallow with maximum depth of 1.1 and 0.9 m, and mean depth of 0.5 and 0.3 m. Their catchment areas are 0,340 and 0,369 km^2, lake area 4220 and 2970 m^2 and water volume 2183 and 1037 m^3, respectively (Nedbalová et al., 2013). Melt water from the surrounding snowfields feed the lakes for a few weeks during the austral summer. The water level in both lakes fluctuated dramatically. Water is mainly lost through evaporation from the ice free water surface. During this period, intense evaporation in both lakes is coupled with macroscopic changes in the littoral belt. The extent of water level fluctuation was documented for lake 1 (Figure 2).

Climate conditions of the Ulu Peninsula are characterized by mean annual air temperatures around –7 °C and mean summer temperatures above 0 °C for up to four months (Láska et al., 2011a). The mean global solar radiation is around 250 W m^{-2} in summer (December-February), with large day-to-day variation affected by extended cyclonic activity in the circumpolar trough and orographic effects over the Antarctic Peninsula (Láska et al., 2011b). The bedrock is composed of two main geological units, namely Cretaceous back-arc basin sediments and mostly subglacial Neogene to Quaternary volcanic rocks (Olivero et al., 1986).

The terrestrial vegetation is limited to non-vascular plants and composed predominantly of lichen and bryophyte tundra. A large number of lakes can be found in this area, formed by glacial erosion and deposition, followed by glacier retreat during the Holocene (Nedbalová et al., 2013).

2.2 Sampling procedures

Lake 1 was sampled on 22 February 2008. In 2009, lake 1 was sampled on 5 January, lake 2 on 12 January. Air temperature at 2 m above ground was measured by an automatic weather station (AWS) located nearby (Figure 1). Incident global solar radiation was monitored with a LI-200 pyranometer (LI-COR, USA) at Mendel Station, located 11 km northwest of the study site (Figure 1). The LI-200 spectral response curve covers wavelengths from 400 to 1100 nm with absolute error typically of ±3% under natural daylight conditions. Global radiation was measured at 10s time interval and stored as 30-min average values, while air temperature was recorded at 1 hour intervals from 1 February 2009 to 30 November 2010. In lake 1, water temperature was monitored from 10 February 2009 to 30 November 2010 at 1 hour intervals using a platinum resistance thermometer with Minikin T data logger (EMS Brno, Czech Republic) installed on the lake bottom.

Conductivity, pH, temperature and dissolved oxygen were measured in situ with a portable meter (YSI 600) at the time the lakes were ice free. Water samples were collected from the surface layer, immediately filtered through a 200-µm polyamide sieve to remove zooplankton and coarse particles. Chlorophyll-a was extracted from particles retained on Whatman GF/F glass microfiber filters according to Pechar (1987). After centrifugation, chlorophyll-a was measured by a Turner TD-700 fluorometer equipped with a non-acidification optical kit. The remaining water was kept frozen until analyzed at the Institute of Hydrobiology (Czech Republic). The chemical analytical methods are given in Nedbalová et al. (2013). The stones covered by photoautotrophic mats – biofilm collected in the field were transported to the Czech Republic in a frozen and/or dry state, documented with stereomicroscope (Bresser, HG 424018) and imaging fluorometer (FluorCam, PSI) and used for a) phytobenthos community description and isolation of dominant species, b) fix for thin section analyses, c) scanning electron and optical microscopy, and d) determination of the structure and chemical composition of calcium carbonate spicules.

2.3 Thin section analyses

Thin section analyses were made to observe both rock substrate and inorganic particles within biofilms. Dry microbial mat were saturated with epoxy resins in vacuum, subsequently cut perpendicularly and saturated again with epoxy resin. The sample was cemented to a glass slide after grinding and polishing, and a thin section was prepared by final sectioning, grinding and polishing to a desired thickness of 50–55 μm. Thin sections of rocks were studied in transmitted (PPL) and polarized (XPL) light (Olympus BX-51M) and documented in transmitted light of a Nikon SMZ-645 optical microscope using NIS-Elements software.

2.4 Biofilm scanning electron and optical microscopy

The morphology of photoautotrophic mats and calcareous spicules was studied using standard methods of scanning electron microscopy (SEM) using back-scattered electrons (BSE) (Jeol JSM-6380, Faculty of Science, Charles University) and optical microscopy (Nikon SMZ-645 using NIS-Elements software). Calcareous spicules were collected directly from the surface of biofilms. Samples studied in SEM were completely dried for 5 months at room temperature, then mounted on stubs with carbon paste and coated with gold prior to photomicrographing.

2.5 Structure and chemical composition of calcium carbonate spicules – EDS and EBSD analyses

The chemical composition of the analyzed spicules was measured by using the Link ISIS 300 system with 10 mm^2 Si-Li EDS detector on a CamScan 3200 scanning electron microscope (Czech Geological Survey, Prague). Analyses were performed using an accelerating voltage of 15 kV, 2 nA beam current, 1 μm beam size and ZAF correction procedures. Natural carbonate standards (calcite, magnesite, rhodochrosite, siderite and smithsonite) were used for standardization. Subsequent structural identification was confirmed by electron backscattered diffraction (EBSD). Identification data and crystallographic orientation measurements were performed on the same scanning electron microscope using an Oxford Instruments Nordlys S EBSD detector. The thick sections used for EBSD applications were prepared by the process of chemo-mechanical polishing using colloidal silica suspension. The acquired EBSD patterns were indexed within Channe l5 EBSD software (Schmidt and Olensen, 1989) applying calcite and aragonite crystallographic models (Effenberger et al., 1981; Caspi et al., 2005). Orientation contrast images were collected from a 4-diodes forescatter electron detector

(FSD) integrated into the Nordlys S camera. EBSD pattern acquisition was carried out at 20 kV acceleration voltage, 3 nA beam current, 33 mm working distance and 70° sample tilt.

3 Results

3.1 General description of the lakes and water chemistry

Pictures and detailed bathymetric parameters of both lakes together with marked lines of water level and the maximum extent of the photosynthetic microbial mat littoral belt in lake 1 are presented in Figure 2.

The physico-chemical characteristics of the lake water for both lakes are given in Table 1. The sampling of lake 1 (pH 7.4–7.9, saturation of oxygen 98.9 %) was performed during cloudy days. Oxygen supersaturation (128%) together with a relatively high pH (8.6) was observed in lake 2 during a sunny day. Conductivity was below 100 μS cm^{-1} in both lakes. The concentrations of dissolved inorganic nitrogen forms were low, whereas the concentration of dissolved reactive phosphorus (SRP) was 19.3 μg L^{-1} in lake 2. Relatively high concentrations of dissolved organic carbon, particulate nutrients and chlorophyll-a were also characteristic for lake 2 (Table 1). Low autotrophic biomass in open water was mostly formed by detached benthic species; no substantial phytoplankton neither floating mats occurred in the lakes. The comparison of the two sampling dates available for lake 1 suggested high fluctuations of dissolved nutrient concentrations.

3.2 Thermal regime

Figure 3a shows the annual variation of daily mean water temperature in lake 1 and of daily mean air temperature in the Solorina Valley (locations of temperature sensors are marked in Figures 1 and 2). Lake 1 was frozen to the bottom from the end of March to the end of October or beginning of November. Air temperatures were frequently lower than water temperatures. Minimum daily mean temperatures on the bottom of the lake were about –12 °C and –10 °C for 2009 and 2010, respectively. Minimum daily mean air temperatures in the same period were between –32 °C and –25 °C. Mean monthly water temperatures in the lake ranged from –10.4 °C (August 2009) to 5.8 °C (February 2010), while monthly mean air temperatures were between –18.7 °C to 0.7 °C. The differences were greater at the beginning of the winter season (June–July), due to a rapid drop of air temperature.

The highest night-day air temperature fluctuations (up to 28 °C) were recorded during the winter months, while the lowest occurred in summer. In contrast, the highest night-day amplitudes of lake water temperature were recorded from November to February, with typical values between 2 °C and 4 °C (Figure 3b).

The course of global solar radiation (Figure 3c) was smooth, with the maximum daily mean of 385 W m^{-2} during clear sky conditions around the summer solstice. Global radiation reached the bottom of both lakes during the ice free period.

The relative frequency of hourly values of lake 1 water and air temperature is shown in Figure S1. Water temperature fluctuation was narrow, ranging from –16 to 8 °C. The bottom of the lake was frozen for most of the year, and the growing season, with water at temperatures from 2 to 8 °C, covered only two-three months (Figure S1a). In contrast to lake water thermal regime, air temperature fluctuations were much wider (from –38 °C to 8 °C) (Figure S1b).

The temperature at the lake bottom was permanently below –4 °C only during the coldest two-three months per year (Fig. S2). The water temperature above 0 °C (liquid phase) was recorded from November to April (139 days in average). The number of days with temperature between 0 and –4 °C remains the same as for liquid water occurrence with small changes in the start and end dates towards to the transition period (February-June and September-November, respectively). In such thermal conditions, the benthic littoral community can be metabolically active.

3.3 Littoral phytobenthos – biofilm community description

The littoral benthic community in lakes 1 and 2 are dominated by the heterocytous cyanobacterium *Calothrix elsteri* Komárek 2011 (Figure 4a), which forms a flat black biofilm on the upper surface of bottom stones (Figure 5), followed by *Hassallia andreassenni* Komárek 2011 and *Hassallia antarctica* Komárek 2011. *Hassallia andreassenni* is associated with calcium precipitation, as described later. *Hassallia antarctica* was found in stone crevices, being only loosely attached to the substrate. Littoral benthic mats – biofilms on stones (Figure 6) are co-dominated on the surface of the blackish cyanobacterial biofilm by the green filamentous and richly-branched alga *Hazenia broadyi* Škaloud et Komárek 2013 (Ulotrichales, Chlorophyceae) (Figure 4b). *Hazenia broadyi* grew in macroscopic colonies producing green spots (Figure 5b,d). Later in the summer season, the green spots connected micro fortified mucilaginous lines (Figure 5c,d). Figure 5a shows the community in early spring whereas Figure 5b,d originated from later summer when the littoral benthic community

was already well developed with a dense coverage of *Hazenia broadyi* green spots. More detailed pictures (Figure 5e,f) documented the structure of the black leather like biofilm with mucilaginous marble on its surface covered by green spots. When the biofilm gets dry, the net of precipitated micro fortified mucilage mixed with soft mineral matter and crystals of calcium carbonate is visible (Figure 5g,h).

Scanning electron micrographs document the structure of the biofilm (Figure 7). Figure 7a shows a lateral view (cross section) of a biofilm with cyanobacterial filaments (*Calothrix elsteri* and *Hassallia andreassenni*). A biofilm upper view (Figure 7b,d) shows the structure of the cyanobacterial-microalgae community producing the mucilaginous micro fortified net of filaments with spots on its surface.

3.4 Inorganic compounds of biofilms

Thin sections, showing both dry biofilms and rock substrate (Figure 8), provided information on various inorganic compounds associated with the soft tissue of the cyanobacterial – microalgal community. These inorganic compounds are represented by (1) allochthonous mineral grains that are overgrown and incorporated by biofilms and (2) calcareous spicules of different sizes ranging from 0.5 mm to 1 cm that are precipitated within the cyanobacterial-microalgal community.

The rock substrate of biofilms is formed by subangular to subrounded pebbles to boulders of basaltic rock, which is dark-grey in colour, compact and usually with a microcrystalline porhyric texture. The rock is not homogenous, but contains numerous ball-like empty voids, which are often partly filled with feldspathoids (Figure 8a). Crystals of plagioclase (feldspar group) and augite (pyroxene group) are easily recognizable in thin sections (Figures 8a–c).

Biofilms are often partly covered with various mineral grains and rock fragments, but all specimens studied also contain these particles incorporated directly within soft cyanobacterial - microalgal filaments (Figure 8a–c).

Mineral grains embedded within biofilms close to the basaltic rock surface are mainly angular to subangular crystal fragments of plagioclase and augite (Figures 8b,c), i.e. the main mineral components of the basaltic rock substrate described above. In the upper part of biofilms, however, partly or fully incorporated grains of quartz occur, being typically rounded or partly rounded (Figures 8a,b). One of the thin sections shows a calcareous spicule in situ and mineral grains within the biofilm (Figures 8c,d).

The structure and morphology of calcareous spicules was studied on SEM (Figure 9). The spicules (see also Methods) show an intensively worn surface (Figure 9a), partial or intense recrystallization (Figures 9a,b) and dissolution (Figure 9b). Crystal facets on the surface and cleavage (crystallographic structural planes) in the interior of the spicules (Figures 9a,b) are typical characteristics of calcium carbonate monocrystals.

A non-recrystallized superficial layer of microcrystalline calcite (e.g., Figure 9b) shows the structure of parallel needle-like calcite microcrystals (Figures 9d–f). Partial corrosion and dissolution of spicules show distinct layering of these needle-like microcrystals (Figure 9d). The layered structure of even partly recrystallized spicules is confirmed in the ring-like structures with a cyanobacterial filament in the centre (Figure 10).

The chemical composition of the studied calcareous spicules determined by FSD corresponds to pure $CaCO_3$. Following chemical composition, calcite and aragonite structural models were applied for the EBSD study focused on structural identification of the crystals forming the spicule. Structural identification of the studied specimen especially prepared for the EBSD study confirmed the absolute agreement between the recorded EBSD patterns and modelled patterns for calcite. The presence of aragonite was not confirmed. FSD images acquired for chemical and orientation contrasts (Figure 10) show a layered structure especially visible in orientation contrast. This feature reflects continual growing processes on layers with very similar crystallographic orientation. Absolute angular differences between individual layers are below 0.8°.

4 Discussion

4.1 Environmental properties

The lakes under study are characterized by a low content of major ions due to their volcanic bedrock and lower marine influence. In comparison with other lakes of this area, the two lakes show no specific lake water chemistry characteristics with moderate SRP and nitrate concentrations frequently below the detection limit (Nedbalová et al., 2013). High pH together with oxygen supersaturation recorded in lake 2 could be associated with high photosynthetic activity of the mats at the time of sampling.

Because water in either liquid or solid form has a large heat storage capacity, it acts as an important buffer to temperature change. Local climatic conditions of shallow freshwater lakes

311 is the principal external factor controlling their ecological functionality. Lake 1 is frozen to
312 the bottom approximately eight-nine months per year. For most of the year, however, the
313 temperature of the littoral and lake bottom is only from –2 to –4 °C. In such conditions, a thin
314 layer of water probably covers the surface of the littoral benthic community that can be
315 metabolically active (Davey et al., 1992). The growing season, with liquid water at
316 temperatures between 2 to 4 °C, covers only two-three months.

317 In regards to heat balance, the studied shallow lakes are pond (wetlands) environments which
318 freeze solid during the winter. This inevitability is a strong habitat-defining characteristic,
319 which places considerable stress on resident organisms (Hawes et al., 1992; Elster, 2002). In
320 summer, they must withstand drying in large parts of the littoral zone due to a considerable
321 drop in water level. In freezing and desiccation resistance studies of freshwater phytobenthos
322 in shallow Antarctic lakes, several ecological measurements have recorded seasonal, diurnal,
323 and year round temperature fluctuations and changes in water state transitions (e.g., Davey,
324 1989; Hawes et al., 1992, Hawes et al., 1999). In localities with steady moisture and nutrient
325 supplies, the abundance and species diversity of algae is relatively high. However, as the
326 severity and instability of living conditions increases (mainly due to changes in mechanical
327 disturbances, desiccation–rehydration and subsequent changes in salinity), algal abundance
328 and species diversity decreases (Elster and Benson, 2004). The speed at which water state can
329 change between liquid, ice, and complete dryness, is one of the most important ecological and
330 physiological factors of these lakes. Studies based on field or laboratory experiments have
331 shown that some cyanobacteria and algae are able to tolerate prolonged periods of desiccation
332 (Pichrtová et al., 2014; Tashyreva and Elster, 2015). It is also obvious that there are
333 strain/species specific differences in the overwintering strategies, and also between
334 strains/species inhabiting different habitats (Davey, 1989; Hawes et al., 1992; Jacob et al.,
335 1992; Šabacká and Elster, 2006; Elster et al., 2008). The ice and snow which cover the lakes
336 for about eight-nine months per year serve as a natural incubator which moderate potential
337 mechanical disturbances and stabilise the thermal regimes of the lakes.

338 ## 4.2 Biodiversity

339 Patterns of endemism and alien establishment in Antarctica are very different across taxa and
340 habitat types (terrestrial, freshwater or marine) (Barnes et al. 2006). Environmental
341 conditions, as well as dispersal abilities, are important in limiting alien establishment (Barnes
342 et al., 2006). Antarctic microbial (cyanobacteria, algae) diversity is still poorly known,

343 although recent molecular and ecophysiological evidence support a high level of endemism
344 and speciation/taxon distinctness (Taton et al., 2003; Rybalka et al., 2009; de Wever et al.,
345 2009; Komárek et al., 2011; Strunecký et al., 2012; Škaloud et al., 2013).

346 The floors of the studied lakes are covered with photosynthetic microbial mats composed of
347 previously described species of heterocytous cyanobacteria, mostly *Calothrix elsteri* Komárek
348 2011 followed by *Hassallia andreassenni* Komárek 2011 and *Hassallia antarctica* Komárek
349 2011 (Komárek et al., 2011). They are co-dominated by a newly described species of green
350 filamentous and richly branched algae *Hazenia broadyi* Škaloud et Komárek 2013
351 (Ulotrichales, Chlorophyceae) (Škaloud et al., 2013). All the previously mentioned recently
352 described species have special taxonomic positions together with special ecology and are
353 considered at present as Antarctic endemic species.

354 The black leather like biofilm with mucilaginous marble on its surface is covered by green
355 spots. These macroscopic structures form mats a few mm thick consisting of the above
356 mentioned species packed in mucilage glued together with fine material. The regular leather
357 biofilm structure with distinct cyanobacterial-microalgal composition and incorporated
358 mineral grains is to our knowledge unique. During the limnological survey of the whole Ulu
359 Peninsula (Nedbalová et al., 2013), this specific biofilm structure was observed only in the
360 two endorheic lakes, although lakes with very similar morphometric and chemical
361 characteristics are found in the area. The mat structure is thus apparently tightly linked to the
362 species composition (Andersen et al., 2011).

363 The low abundance of benthic diatoms in the lakes is unusual, but not unprecedented as there
364 are other areas in Antarctica where diatoms are scarce or absent (Broady, 1996, Wagner et al.,
365 2004). The reason underlying the absence of diatoms is not immediately obvious, because
366 diatoms are quite a common and frequently dominant component of microbial communities in
367 most freshwater habitats of the Ulu Peninsula, James Ross Island (Kopalová et al., 2013).
368 Local geographical separation of lakes 1 and 2 together with founder effect may have
369 precluded successful colonization by the subset of diatoms that are common in the
370 surrounding freshwater habitats. Although it has long been held that diatoms are dispersed
371 widely, some recent reports document very small scale microbial distributions and endemism
372 (Kopalová et al., 2012; Kopalová et al., 2013).

4.3 Inorganic compounds of biofilms

Based on the character of the rock substrate and lake sediments it is suggested, that one of the main prerequisites for existence of this cyanobacterial-microalgal community producing unusual biogenic calcite structures is; (1) flat and stable substrate in both lakes and (2) low sedimentation rate.

The substrate for biofilms is composed of boulders and pebbles of the stony littoral zone, petrographically corresponding to compact and massive basaltoids (Smellie et al., 2008; Svojtka et al., 2009). Rounded or sub-rounded quartz grains that are incorporated ("trapped") within biofilms cannot originate from basaltic volcanic rocks forming the bottom of both lakes and substrate of the studied biofilms. This is evidenced by the petrographic character of the basaltoids, which do not contain any quartz. The presence of abraded quartz grains in lake 1 and 2 can be easily explained by wind transport (e.g., Shao, 2008).

The specific cyanobacterial-microalgal community described above can prosper in the two shallow endorheic lakes, because of low sedimentation rates resulting from minor water input. Low sedimentary input is the main necessary ecological parameter which facilitates the existence of this special microbial community. The community is, however, well adapted to seasonally elevated sedimentation rates coming from frequent and intense winds. During wind storms, the wind is carrying a relatively large amount of small mineral grains and rock microfragments (intense eolic erosion; e.g., Shao (2008) and references therein). These grains and particles are usually derived from erosion of the rocks either in the very close vicinity of the locality (weathering of basaltic rocks), but mainly come from remote locations where especially Upper Cretaceous marine sedimentary sequences are outcropping (Smellie et al., 2008; Svojtka et al., 2009). Even elevated amounts of mineral grains transported into the lake by wind do not stop the growth of cyanobacterial-microalgae biofilms, due to their ability of incorporating and "trapping" mineral grains within the living tissue (Riding, 2011).

This study has shown that inorganic substances precipitated by microbial lithogenetic processes are exclusively represented by calcite spicules. Precipitation of carbonate outside of microorganisms during photosynthesis as a mechanism of carbonate construction was described for many filamentous cyanobacterial species (Schneider and Le Campion-Alsumard, 1999). However, the biogenic calcite structures in both lakes are quite different to any microbially mediated structures yet described from modern environments (Kremer et al., 2008; Couradeau et al., 2011) and also to structures formed by abiotic precipitation (e.g., Vogt and Corte, 1996). Although there are many lakes with thick mats and similar chemical

406 characteristics on the Ulu Peninsula, the calcite spicules were found exclusively in the two
407 endorheic lakes. We believe that their formation is linked to the specific photoautotrophic
408 mats present in the lakes. From Figures 6g,h it is clearly visible that the calcareous
409 organosedimentary structures keep contours of viable photosynthetic microbial mat after
410 desiccation or calcite spicules precipitation. More specifically, the co-dominance of a green
411 microalga is unique since mats in Antarctic lakes are most frequently formed by filamentous
412 cyanobacteria (Vincent and Laybourn-Parry 2008). Therefore, we hypothesise that the more
413 rapid photosynthesis rate of *Hazenia* in comparison with cyanobacteria may induce conditions
414 necessary for carbonate precipitation in the lakes (Schneider and Le Campion-Alsumard,
415 1999; Vincent, 2000). However, some role of abiotic precipitation of calcite is also possible.
416 From our observations we cannot clearly decide if the winter abiotic calcite precipitation
417 accompany microbial lithogenetic processes.

418 Although we interpret the tubular hollow observed in the centre of some spicules as the result
419 of the presence of cyanobacterial filament during the process of crystallization, such
420 structures may form also as the result of abiotic precipitation of calcite (Vogt and Corte, 1996;
421 Fan and Wang, 2005).

422 It is striking that some calcite spicules probably exhibit recrystallization, forming spicules
423 with the structure of calcite monocrystals. However, these spicules could be also interpreted
424 as primary structures: mesostructured carbonate crystals formed through highly oriented
425 growth of micro/nanocrystals and characterized by a specific surface texture (Fig. 9a–b).
426 There is already evidence that some biominerals including calcite are mesocrystals (Cölfen
427 and Antonietti, 2005) and the importance of extracellular polymeric substances for the
428 formation of some types of carbonate precipitates was documented (Pedley et al., 2009).

429 Determining the structure and material of precipitated inorganic substances brought another
430 relevant question: "Do calcite spicules have fossilisation potential"? Microcrystalline calcite
431 forming the recrystallized spicule is a typical material of calcite shells of fossil invertebrates
432 (e.g., Vodrážka, 2009). Although calcite fossils may be partly or completely dissolved during
433 diagenetical processes in the fossil record (e.g., Schneider et al., 2011; Švábenická et al.,
434 2012), their preservation potential is relatively high. Therefore, we expect to find fossil and/or
435 sub-fossil calcite spicules from the Quaternary lake sediments of the studied area.

436

437 **Acknowledgements**

This study was conducted during two Czech Antarctic research expeditions of the authors (J.E., L.N., R.V., K.L., J.K.) to the J. G. Mendel station in 2008 and 2009 (headed by Prof. Miloš Barták). We are indebted particularly to the staff and scientific infrastructure of the station. The study was supported by the Ministry of Education, Youth and Sports of the Czech Republic (CzechPolar LM2010009 and RVO67985939). R.V. has been funded through a Research and Development Project of the Ministry of Environment of the Czech Republic No. SPII 1a9/23/07 and by a project of the Czech Geological Survey No. 338900. K.L. was supported by a project of Masaryk University MUNI/A/0902/2012 "Global environmental changes and their impacts" (GlobE). The technical work in laboratories was performed by Jana Šnokhousová and Dana Švehlová.

References

Andersen, D. T., Sumner, D. Y., Hawes, I., Webster-Brown, J., and McKay, C. P.: Discovery of large conical stromatolites in Lake Untersee, Antarctica. Geobiology, 9, 280–293, doi: 10.1111/j.1472-4669.2011.00279.x, 2011.

Arp, G., Reimer, A., and Reitner, J.: Photosynthesis-induced biofilm calcification and calcium concentrations in Phanerozoic oceans. Science, 392, 1701, doi: 10.1126/science.1057204, 2001.

Barnes, D. K. A., Hodgson, D. A., Convey, P., Allen, C. S., and Clarke, A.: Incursion and excursion of Antarctic biota: past, present and future. Global Ecol. Biogeogr., 15, 121–142, doi: 10.1111/j.1466-822x.2006.00216.x, 2006.

Broady, P. A.: Diversity, distribution and dispersal of Antarctic terrestrial algae. Biodiv. Conserv., 5, 1307–1335, doi: 10.1007/BF00051981, 1996.

Caspi, E. N., Pokroy, B., Lee, P. L., Quintana, J. P., and Zolotoyabko, E.: On the structure of aragonite. Acta Crystallogr., B 61, 129–132, doi: 10.1107/S0108768105005240, 2005.

Clark, I. D. and Lauriol, B.: Aufeis of the Firth River basin, Northern Yukon Canada: insights to permafrost hydrology and karst. Arct. Alp. Res., 29, 240–252, doi: 10.2307/1552053, 1997.

Courty, M. A., Marlin, C., Dever, L., Tremblay, P., and Vachier, P.: The properties, genesis and environmental significance of calcite pendents from the high Arctic (Spitsbergen). Geoderma, 61, 71–102, doi: 10.1016/0016-7061(94)90012-4, 1994.

Couradeau, E., Benzerara, K., Moreira, D., Gérard, E., Kaźmierczak, J., Tavera, R. and López-García, P.: Prokaryotic and eukaryotic community structure in field and cultured microbialites from the alkaline lake Alchichica (Mexico). PloS ONE, 6, 1–15, doi: 10.1371/journal.pone.0028767, 2011.

Cölfen, H. and Antonietti, M.: Crystal design of calcium carbonate microparticles using double-hydrophilic block copolymers. Langmuir, 14, 582–589, doi: 10.1021/la970765t, 1998.

Cölfen, H. and Antonietti, M.: Mesocrystals: inorganic superstructures made by highly parallel crystallization and controlled alignment. Angew. Chem. Int. Ed., 44, 5576–5591, doi: 10.1002/anie.200500496, 2005.

Davies, B. J., Glasser, N.F., Carrivick, J. L., Hambrey, M. J., Smellie, J. L., and Nývlt, D.: Landscape evolution and ice-sheet behavior in a semi-arid polar environment: James Ross Island, NE Antarctic Peninsula. Special publication. Geological Society of London, doi: 10.1144/SP381.1, 2013.

Davey, M. C.: The effect of freezing and desiccation on photosynthesis and survival of terrestrial Antarctic algae and cyanobacteria. Polar Biol., 10, 29–36, 1989.

Davey, M. C., Pickup, J., and Block, W.: Temperature variation and its biological significance in fellfield habitats on a maritime Antarctic island. Antarct Sci., 4, 383–388, 1992.

De Wever, A., Leliaert, F., Verleyen, E., Vanormelingen, P., Van der Gucht, K., Hodgson, D. A., Sabbe, K., and Vyverman, W.: Hidden levels of phylodiversity in Antarctic green algae: further evidence for the existence of glacial refugee. P. Roy. Soc. B-Biol. Sci., 276, 3591–3599, doi: 10.1098/rspb.2009.0994, 2009.

Effenberger, H., Mereiter, K., and Zemann, J.: Crystal structure refinements of magnesite, calcite, rhodochrosite, siderite, smithsonite and dolomite, with discussion of some aspects of the stereochemistry of calcite-type carbonates. Z. Kristallogr., 156, 233–243, 1981.

493 Elster, J.: Ecological classification of terrestrial algal communities of polar environment, in:
494 GeoEcology of terrestrial oases, edited by: Beyer, L. and Boelter, M., 303–319. Ecological
495 Studies, Springer-Verlag, Berlin, Heidelberg, 2002.

496 Elster, J. and Benson, E. E.: Life in the polar terrestrial environment with a focus on algae and
497 cyanobacteria, in: Life in the frozen state, edited by: Fuller, B., Lane, N. and Benson E. E.,
498 111–149. Taylor and Francis, London, doi: 10.1201/9780203647073.ch3, 2004.

499 Elster, J., Degma, P., Kováčik, Ľ., Valentová, L., Šrámková, K., and Pereira, A. B.: Freezing
500 and desiccation injury resistance in the filamentous green alga Klebsormidium from the
501 Antarctic, Arctic and Slovakia. Biologia, 63, 839–847, doi: 10.2478/s11756-008-0111-2,
502 2008.

503 Fairchild, I. J., Bradby, B., and Spiro, B.: Carbonate diagenesis in ice. Geology, 21, 901–904,
504 doi: 10.1130/0091-7613(1993)021<0901:CDII>2.3.CO;2, 1993.

505 Fan, Y.W. and Wang, R.Z: Submicrometer-sized vaterite tubes formed through nanobubble-
506 templated crystal growth. Adv. Mater., 17, 2384–2388, doi: 10.1002/adma.200500755, 2005.

507 Jacob, A., Wiencke, C., Lehmann, H., and Krist, G. O.: Physiology and ultrastructure of
508 desiccation in the green alga Prasiola crispa from Antarctica. Bot. Mar., 35, 297–303, doi:
509 10.1515/botm.1992.35.4.297, 1992.

510 Johnson, J. S., Bentley, M. J., Roberts, S. J., Binnie, S. A., and Freeman, S. P. H. T.:
511 Holocene deglacial history of the northeast Antarctic Peninsula – A review and new
512 chronological constraints. Quaternary Sci. Rev., 30, 3791–3802, doi:
513 10.1016/j.quascirev.2011.10.011, 2011.

514 Hawes, I., Smith, R., Howard-Williams, C., and Schwarz, A. M.: Environmental conditions
515 during freezing, and response of microbial mats in ponds of the McMurdo Ice Shelf,
516 Antarctica. Antarct. Sci., 11, 198–208, 1999.

517 Hawes, I., Howard-Williams, C., and Vincent, W. F.: Desiccation and recovery of Antarctic
518 cyanobacterial mats. Polar Biol., 12, 587–594, 1992.

519 Hawes, I., Moorhead, D., Sutherland, D., Schmeling, J., and Schwarz, A. M.: Benthic primary
520 production in two perennially ice-covered Antarctic lakes: pattern of biomass accumulation
521 with a model of community metabolism. Antarct.Sci., 13, 18–27, 2001.

522 Komárek, J. and Elster, J.: Ecological background of cyanobacterial assemblages of the
523 northern part of James Ross Island, NW Weddell Sea, Antarctica. Pol. Polar Res., 29, 17–32,
524 2008.

525 Komárek, J., Nedbalová, L., and Hauer, T.: Phylogenetic position and taxonomy of three
526 heterocytous cyanobacteria dominating the littoral of deglaciated lakes, James Ross Island,
527 Antarctica. Polar Biol., 35, 759–774, doi: 10.1007/s00300-011-1123-x, 2011.

528 Komárek, J., Bonaldo, G. D., Fatima, F. M., and Elster, J.: Heterocytous cyanobacteria of the
529 Ulu Peninsula, James Ross Island, Antarctica. Polar Biol., 38, 475–492, doi: 10.1007/s00300-
530 014-1609-4, 2015.

531 Kopalová, K., Veselá, J., Elster, J., Nedbalová, L., Komárek, J., and Van de Vijver, B.:
532 Benthic diatoms (Bacillariophyta) from seepages and streams on James Ross Island (NW
533 Weddell Sea, Antarctica). Plant Ecol. Evol., 145, 1–19, doi: 10.5091/plecevo.2012.639, 2012.

534 Kopalová, K., Nedbalová, L., Nývlt, D., Elster, J., and Van de Vijver, B.: Diversity, ecology
535 and biogeography of the freshwater diatom communities from Ulu Peninsula (James Ross
536 Island, NE Antarctic Peninsula). Polar Biol., 36, 933–948, doi: 10.1007/s00300-013-1317-5,
537 2013.

538 Kremer, B., Kaźmierczak, J., and Stal, L. J.: Calcium carbonate precipitation in cyanobacteria
539 mats from sandy tidal flats of the North Sea. Geobiology, 6, 46–56, doi: 10.1111/j.1472-
540 4669.2007.00128.x, 2008.

541 Láska, K., Barták, M., Hájek, J., Prošek, P., and Bohuslavová, O.: Climatic and ecological
542 characteristics of deglaciated area of James Ross Island, Antarctica, with a special respect to
543 vegetation cover. Czech Polar Reports, 1, 49–62, 2011a.

544 Láska, K., Budík, L., Budíková, M., and Prošek, P.: Method of estimating of solar UV
545 radiation in high-latitude locations based on satellite ozone retrieval with improved algorithm.
546 Int. J. Remote Sens., 32, 3165–3177, doi: 10.1080/01431161.2010.541513, 2011b.

Lepot, K., Compère, P., Gérard, E., Namsaraev, Z., Verleyen, E., Tavernier, I., Hodgson, D. A., Vyverman, W., Gilbert, B., and Javaux, E. J. : Organic and mineral imprints in fossil photosynthetic mats of an East Antarctic lake. Geobiology, 12, 424–450, doi: 10.1111/gbi.12096, 2014.

Nakai, N., Wada, H., Kiyoshu, Y., and Takimoto, M.: Stable isotope studies on the origin and geological history of water and salts in the Lake Vanda area, Antarctica. Geochem. J., 9, 7–24, 1975.

Nedbalová, L., Nývlt, D., Kopáček, J., Šobr, M., and Elster, J.: Freshwater lakes of Ulu Peninsula, James Ross Island, north-east Antarctic Peninsula: origin, geomorphology, and physical and chemical limnology. Antarct. Sci., 25, 358–372, doi: 10.1017/S0954102012000934, 2013.

Ng, F. and Hallet, B.: Patterning mechanisms in subglacial carbonate dissolution and deposition. J. Glaciol., 48, 386–400, 2002.

Nývlt, D., Košler, J., Mlčoch, B., Mixa, P., Lisá, L., Bubík, M., and Hendriks, B. W. H.: The Mendel Formation: evidence for late Miocene climatic cyclicity at the northern tip of the Antarctic Peninsula. Palaeogeogr. Palaeocl., 299, 363–394, 10.1016/j.palaeo.2010.11.017, 2011.

Olivero, E. B., Scasso, R. A., and Rinaldi, C. A.: Revision of the Marambio Group, James Ross Island, Antarctica. Instituto Antartico Argentino, Contribución, 331, 1–28, 1986.

Øvstedal, D. O., and Lewis Smith, R. I.: Lichens of Antarctica and South Georgia: A guide to their identification and ecology. Studies in Polar Research, Cambridge University Press, Cambridge, 411 pp, 2001.

Pechar, L.: Use of acetone:methanol mixture for the extraction and spectrophotometric determination of chlorophyll a in phytoplankton. Archiv für Hydrobiologie/Supplement, Algological Studies, 46, 99–117, 1987.

Pedley, M., Rogerson, M., and Middleton, R.: Freshwater calcite precipitates from in vitro mesocosm flume experiments: a case for biomediation of tufas. Sedimentology 56, 511-527, doi: 10.1111/j.1365-3091.2008.00983.x, 2009.

575 Pichrtová, M., Hájek, T., and Elster, J.: Osmotic stress and recovery in field populations of
576 Zygnema sp. Zygnematophyceae, Streptophyta) on Svalbard (High Arctic) subjected to
577 natural dessication. FEMS Microbiol. Ecol., 89, 270–280, doi:10.1111/1574-6941.12288,
578 2014.

579 Rabassa, J., Skvarca, P., Bertani, L., and Mazzoni, E.: Glacier inventory of James Ross and
580 Vega Islands, Antarctic Peninsula. Ann. Glaciol., 3, 260–264, 1982.

581 Reid, P., Dupraz, C., Visscher, P., and Sumner, D.: Microbial processes forming marine
582 stromatolites, in: Fossil and recent biofilms – a natural history of life on Earth, edited by:
583 Krumbein, W.E., Peterson, D.M., and Zavarzin, G. A., 103–118. Kluwer Academic
584 Publishers, London, 2003.

585 Riding, R.: Microbialities, stromatolites, and thrombolites, in: Encyclopedia of Geobiology,
586 edited by: Reitner, J. and Thiel, V., 635–654, Encyclopedia of Earth Science Series, Springer,
587 Heidelberg, 2011.

588 Rybalka, N., Andersen, R. A., Kostikov, I., Mohr, K. I., Massalski, A., Olech, M., and Friedl,
589 T.: Testing for endemism, genotypic diversity and species concepts in Antarctic terrestrial
590 microalgae of the Tribonemataceae (Stramenophiles, Xanthophyceae). Environ. Microbiol.,
591 11, 554–565, doi: 10.1111/j.1462-2920.2008.01787.x, 2009.

592 Šabacká, M. and Elster, J.: Response of cyanobacteria and algae from Antarctic wetland
593 habitats to freezing and desiccation stress. Polar Biol., 30, 31–37, doi: 0.1007/s00300-006-
594 0156-z, 2006.

595 Shao, Y.: Physics and Modelling of Wind Erosion. Atmospheric and Oceeanographic
596 Sciences Library 37. 2nd Edition. Springer, Heidelberg. 456 pp, 2008.

597 Schieber, J.: Microbial mats in terrigenous clastics: the challenge of identification in the rock
598 record. Palaios, 14, 3–12, doi: 10.2307/3515357, 1999.

599 Schmidt, N. H. and Olensen, N. O.: Computer-aided determination of crystal-lattice
600 orientation from electron-channeling patterns in the SEM. Can. Mineral., 28, 15–22, 1989.

601 Schneider, S. and Le Campion-Alsumard, T.: Construction and destruction of carbonates by
602 marine and freshwater cyanobacteria. Eur. J. Phycol., 34, 417–426, doi:
603 10.1017/S0967026299002280, 1999.

604 Schneider, J., Niebuhr, B., Wilmsen, M., and Vodrážka, R.: Between the Alb and the Alps –
605 The fauna of the Upper Cretaceous Sandbach Formation (Passau region, southeast Germany).
606 Bull. Geosci., 86, 785–816, doi: 10.3140/bull.geosci.1279, 2011.

607 Škaloud, P., Nedbalová, L., Elster, J., and Komárek, J.: A curious occurrence of Hazenia
608 broadyi spec. nova in Antarctica and the review of the genus Hazenia (Ulotrichales,
609 Chlorophyceae). Polar Biol., 36, 1281–1291, doi: 10.1007/s00300-013-1347-z, 2013.

610 Smellie, J. L., Johnson, J. S., McIntosh, W. C., Esser, R., Gudmundsson, M. T., Hambrey, M.
611 J., and Van Wyk de Vries, B.: Six million years of glacial history recorded in volcanic
612 lithofacies of the James Ross Island Volcanic Group, Antarctic Peninsula. Palaeogeogr.
613 Palaeocl., 260, 122–148, doi: 10.1016/j.palaeo.2007.08.011, 2008.

614 Strunecký, O., Elster, J., and Komárek, J.: Molecular clock evidence for survival of Antarctic
615 cyanobacteria (Oscillatoriales, Phormidium autumnale) from Paleozoic times. FEMS
616 Microbiol. Ecol., 82, 482–490, doi: 10.1111/j.1574-6941.2012.01426.x, 2012.

617 Sutherland, D. and Hawes, I.: Annual growth layers as proxies for past growth conditions for
618 benthic microbial mats in a perennially ice-covered Antartic lake. FEMS Microbiol. Ecol., 67,
619 279–292, doi: 10.1111/j.1574-6941.2008.00621.x, 2009.

620 Švábenická, L., Vodrážka, R., and Nývlt, D.: Calcareous nannofossils from the Upper
621 Cretaceous of northern James Ross Island, Antarctica. Geol. Q., 56, 765–772, doi:
622 10.7306/gq.1053, 2012.

623 Svojtka, M., Nývlt, D., Muramaki, M., Vávrová, J., Filip, J., and Mixa, P.: Provenance and
624 post-depositional low-temperature evolution of the James Ross Basin sedimentary rocks
625 (Antarctic Peninsula) based on fission track analysis. Antarct. Sci., 21, 593–607, doi:
626 10.1017/S0954102009990241, 2009.

627 Tashyreva, D. and Elster, J.: The limits of desiccation tolerance of Arctic Microcoleus strains
628 (Cyanobacteria) and environmental factors inducing desiccation tolerance. Front. Microbiol.,
629 doi: 10.3389/fmicb.2015.00278, 2015.

630 Taton, A., Grubisic, S., Brambilla, E., de Wit, R., and Wilmotte, A.: Cyanobacterial diversity
631 in natural and artificial microbial mats of Lake Fryxell (McMurdo Dry Valleys, Antarctica): a
632 morphological and molecular approach. Appl. Environ. Microb., 69, 5157–5169, doi:
633 10.1128/AEM.69.9.5157-5169.2003, 2003.

634 Turner, J., Barrand, N. E., Bracegirdle, T. J., Convey, P., Hodgson, D. A., Jarvis, M., Jenkins,
635 A., Marshall, G., Meredith, M. P., Roscoe, H., Shanklin, J., French, J., Goosse, H.,
636 Guglielmin, M., Gutt, J., Jacobs, S., Kennicutt, M. C., Valerie Masson-Delmotte, II.,
637 Mayewski, P., Navarro, F., Robinson, S., Scambos, T., Sparrow, M., Summerhayes, C.,
638 Speer, K., and Klepikov, A.: Antarctic climate change and the environment: an update. Polar
639 Rec., 50, 237–259, doi: 10.1017/S0032247413000296, 2014.

640 Vincent, W. F. and Laybourn-Parry, J. (Eds.): Polar lakes and rivers. Oxford University Press,
641 Oxford, 346 pp, doi: 10.1093/acprof:oso/9780199213887.001.0001, 2008.

642 Vincent, W. F.: Cyanobacterial dominance in polar regions, in: The Ecology of
643 Cyanobacteria, edited by: Whitton B. A. and Potts, M., 321–340. Kluwer Academic
644 Publishers, the Netherlands, 2000.

645 Vodrážka, R.: A new method for the extraction of macrofossils from calcareous rocks using
646 sulphuric acid. Palaeontology, 52, 187–192, doi: 10.1111/j.1475-4983.2008.00829.x, 2009.

647 Vogt, T. and Corte, A. E.: Secondary precipitates in Pleistocene and present cryogenic
648 environments (Mendoza Precordillera, Argentina, Transbaikalia, Siberia, and Seymour Island
649 Antarctica). Sedimentology, 43, 53–64, doi: 10.1111/j.1365-3091.1996.tb01459.x, 1996.

650 Wadham, J. L., Tranter, M., and Dowdeswell, J. A.: Hydrochemistry of meltwaters draining a
651 polythermal-based, high-Arctic glacier, south Svalbard: II. Winter and early spring. Hydrol.
652 Process., 14, 1767–1786, doi: 10.1002/1099-1085(200007)14:10<1767: AID-
653 HYP103>3.0.CO;2-Q, 2000.

Wagner, B., Cremer, H., Hulzsch, N., Gore, D., and Melles, M.: Late Pleistocene and Holocene history of Lake Terrasovoje, Amery Oasis, East Antarctica, and its climatic and environmental implications. J. Paleolimnol., 32, 321–339, doi: 10.1007/s10933-004-0143-8, 2004.

Walter, M.: Stromatolites. Elsevier Science Ltd., Amsterdam, the Nederlands, 1976, 790 pp.

Wharton, R. A., Parker, B. C., Simmons, G. M., and Love, F. G.: Biogenic calcite structures forming in Lake Fryxell, Antarctica. Nature, 295, 403–405, doi: 10.1038/295403a0, 1982.

Wharton, R.: Stromatolitic mats in Antarctic lakes, in: Phanerozoic Stromatolites, II, edited by: Bertrand-Safari, J. and Monty, C., 53–70, Springer, New York, USA, doi: 10.1007/978-94-011-1124-9_3, 1994.

Yamamoto, A., Tanabe, K., and Isozaki, Y.: Lower Cretaceous freshwater stromatolites from northern Kyushu, Japan. Paleontol. Res., 13, 139–149, 10.2517/1342-8144-13.2.139, 2009.

683 Table 1. Physico-chemical characteristics and chlorophyll-a concentrations in lake water.
684 Samples were collected from surface of lakes. ND – not determined, ANC – acid
685 neutralization capacity, PN – particulate nitrogen, DP – dissolved phosphorus, PP –
686 particulate phosphorus, SRP – dissolved reactive phosphorus, DOC – dissolved organic
687 carbon, PC – particulate carbon, * – laboratory values.

Lake		Green 1		Green 2
Date		22.2.2008	5.1.2009	12.1.2009
Temperature	°C	3.5	ND	12.3
O_2	mg L^{-1}	13.1	ND	13.7
O_2 saturation	%	98.7	ND	128.0
pH		7.9	7.4*	8.6
Conductivity (25 °C)	µS cm^{-1}	54	48*	97
ANC	mmol L^{-1}	236	246	455
Na^+	mg L^{-1}	4.7	5.9	12.5
K^+	mg L^{-1}	0.24	0.29	0.60
Ca^{2+}	mg L^{-1}	2.12	1.26	2.32
Mg^{2+}	mg L^{-1}	1.24	0.77	1.65
SO_4^{2-}	mg L^{-1}	1.74	1.33	2.60
Cl^-	mg L^{-1}	5.3	5.1	10.6
NO_3-N	µg L^{-1}	<5	11	<5
NO_2-N	µg L^{-1}	0.6	0.2	0.1
NH_4-N	µg L^{-1}	6	<5	<5
PN	µg L^{-1}	20	50	73
DP	µg L^{-1}	7.8	20.2	30.4
PP	µg L^{-1}	4.6	5.9	11.7
SRP	µg L^{-1}	4.0	11.6	19.3
DOC	mg L^{-1}	1.25	1.13	2.17
PC	mg L^{-1}	0.13	0.41	1.33
Si	mg L^{-1}	1.45	0.87	2.85
chl-*a*	µg L^{-1}	0.9	ND	6.0

688

689

Figure captions

Figure 1. Location of lake 1 and 2 and air temperature measurements (ASW) in the Solorina Valley.

Figure 2. Bathymetric parameters of lake 1 (a) and 2 (b) together with marked lines of water level and maximum extent of the photosynthetic microbial mat littoral belt in lake 1.

Figure 3. a – annual variation of daily mean water temperature in lake 1 (L1water) and annual variation of daily mean air temperature in the Solorina Valley (SV air), b – diurnal temperature amplitudes in lake 1 (L1 water) and diurnal air temperature amplitudes in the Solorina Valley (SV air), respectively. c – daily mean global radiation at Mendel Station. All parameters measured from February 2009 to November 2010.

Figure 4. Dominant species in the photoautotrophic mats.

a – *Calothrix elsteri*,

b – *Hazenia broadyi*

Figure 5. Photoautotrophic mats in lakes 1 and 2.

a,b – rapid development of the mat in January 2009 (lake 1). The two photos show the mat at a one week interval, note the growth of gelatinous clusters of densely agglomerated filaments of the green alga *Hazenia broadyi*,

c,d – fully developed mats with mosaic-like structures on the surfaces of stones in the littoral zone of lake 2,

e,f – detail,

g – drying of the mat in the littoral zone leaves a characteristic structure on the surface of stones,

h – calcium carbonate spicule in situ (arrowed)

718 Figure 6. Photoautotrophic mat covering a stone visualized using imaging fluorometry.

719 a – upper view,

720 b – lateral view

721

722 Figure 7. SEM macrographs showing the structure of the dried mat in the lakes.

723 a – transversal section of the mat with visible cyanobacterial filaments,

724 b – surface structure of the mat, the position of cyanobacterial filaments incorporated within
725 mucilaginous matrix is indicated by arrows,

726 c – general view of the surface structure of the mat with the net formed by mucilage (compare
727 with Fig. 7d),

728 d – detail of the same mucilaginous structure

729

730 Figure 8. Perpendicular thin sections of rock substrate covered by dry biofilms (recorded
731 under cross polars). Note that biofilms are partly detached from the surface of the rock due to
732 complete drying of the sample.

733 a – conspicuous U-shaped empty void (arrowed "2") near the surface of basaltic rock partly
734 infilled with crystals of feldspathoids (tectosilicate minerals, arrowed "1"); empty void is
735 bridged by biofilm (arrowed "3") with partly incorporated mineral clasts, represented by semi-
736 rounded quartz grains (arrowed "4"),

737 b – rather thick biofilm with numerous incorporated mineral grains. Note that close to the
738 rock substrate the angular grains of plagioclase (feldspar group) and augite (pyroxene group)
739 dominate, being derived from basaltoids, whereas close to the surface rounded grains of
740 quartz occur (arrowed),

741 c – in situ calcium carbonate spicule penetrating biofilm and surrounded by incorporated
742 grains of feldspars (two arrows on the left) and pyroxene (arrow on the right),

743 d – close up of the same calcium carbonate spicule with a cyanobacterial filament in its centre

744

Figure 9. SEM macrographs showing the morphology of partly recrystallized calcium carbonate spicules. Spicules were washed away from the living tissue and collected directly from the surface of biofilms, although residence time on the bottom cannot be determined.

a – calcareous spicule showing specific surface texture ("worn surface") and complete recrystallization of the spicule interior. The spicule shows crystal facets on the surface and cleavage (crystallographic structural planes) in the interior (arrowed) – i.e. typical characteristics of calcium carbonate monocrystal,

b – detail of previous image; two parallel systems of deep furrows on the surface are crystallographic structural planes of calcite monocrystal; remnants of a superficial layer of microcrystalline calcite are, however, preserved in places on the surface of the crystal (arrowed),

c–f – poorly recrystallized spicule, formed mainly by microcrystalline calcite,

c – lateral view of the spicule,

d – detail of the surface showing corrosion of needle-like calcite microcrystals with distinct layering,

e – parallel needle-like calcite microcrystals on the surface of the central part of the spicule,

f – tops of parallel needle-like calcite microcrystals on the surface of the terminal part of the spicule; the view is perpendicular with respect to the previous macrograph

Figure 10. FSD image of a transversely sectioned, partly recrystallized calcite spicule acquired in (a) chemical contrast, (b) orientation contrast

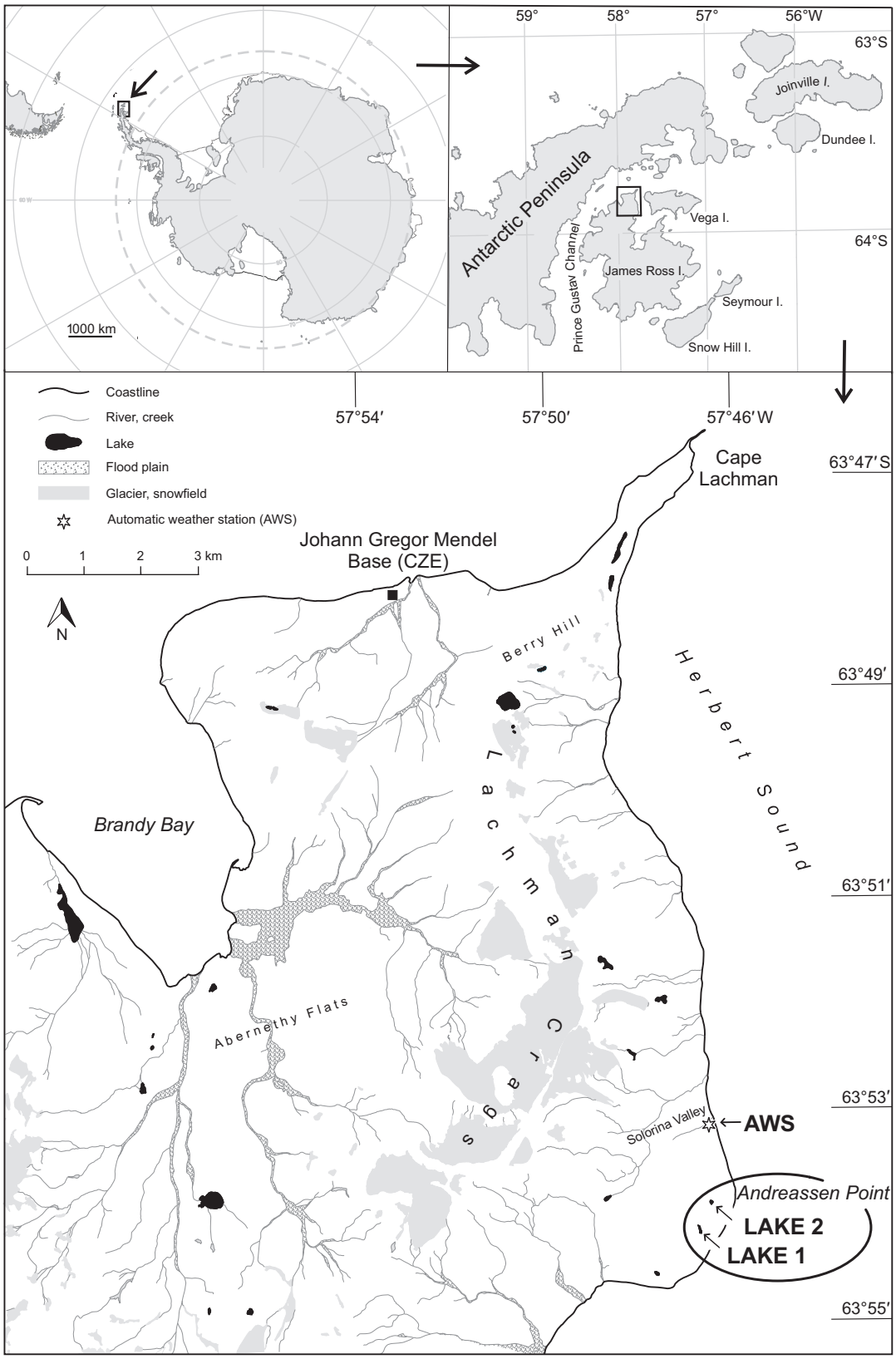
59°
58°
57°
56°W
63°S
Joinville I.
Dundee I.
Antarctic Peninsula
Vega I.
64°S
Prince Gustav Channel
James Ross I.
Seymour I.
Snow Hill I.
1000 km
Coastline
River, creek
Lake
Flood plain
Glacier, snowfield
Automatic weather station (AWS)
0 1 2 3 km
N
57°54′
57°50′
57°46′W
63°47′S
Cape Lachman
Johann Gregor Mendel Base (CZE)
Berry Hill
Herbert Sound
63°49′
Lachman Crags
Brandy Bay
Abernethy Flats
63°51′
63°53′
Solorina Valley
AWS
Andreassen Point
LAKE 2
LAKE 1
63°55′

Fig. 1

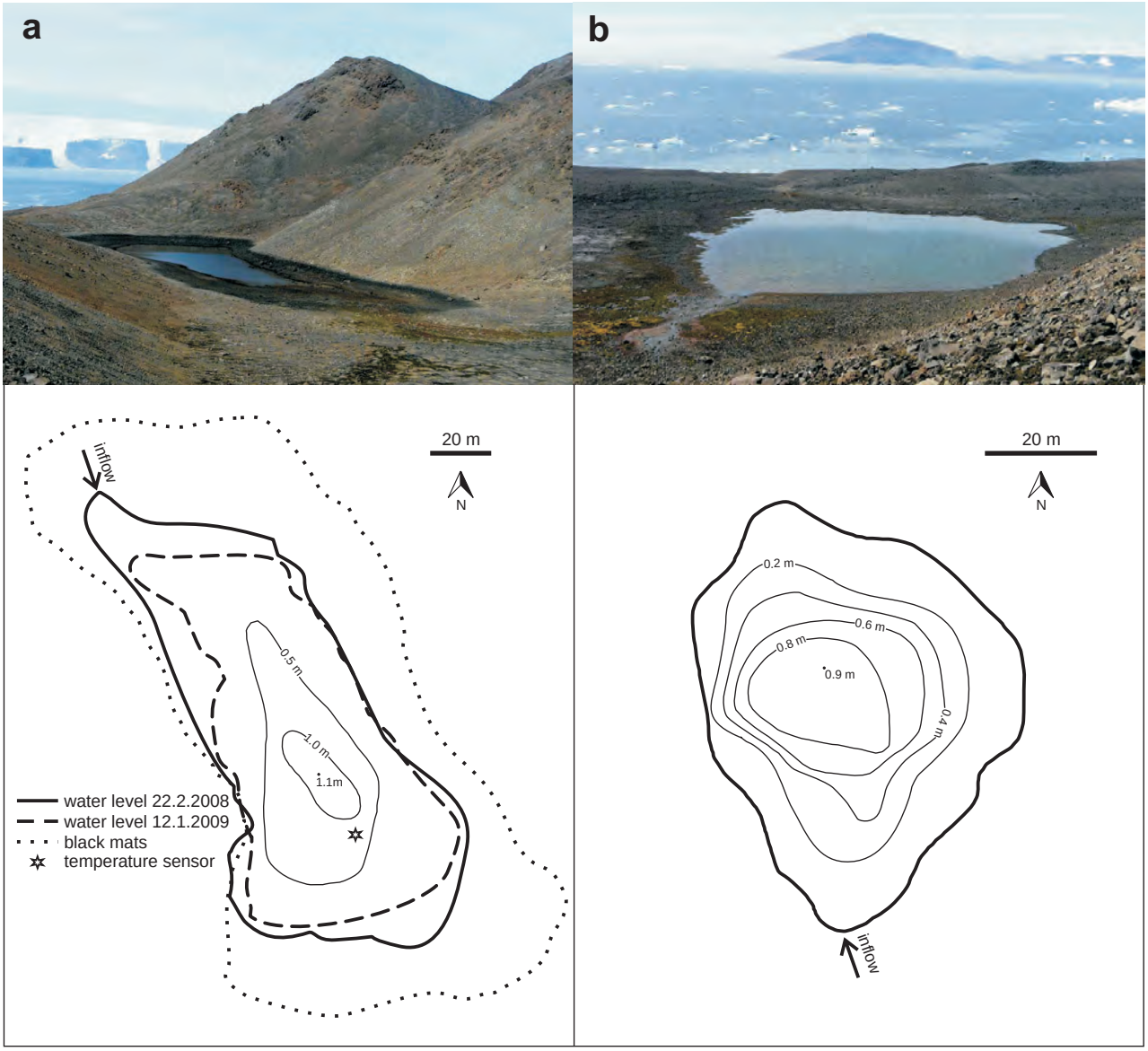
a
b
20 m
N
inflow
0.5 m
1.0 m
1.1m
water level 22.2.2008
water level 12.1.2009
black mats
temperature sensor
20 m
N
0.2 m
0.6 m
0.8 m
0.9 m
0.4 m
inflow

Fig. 2

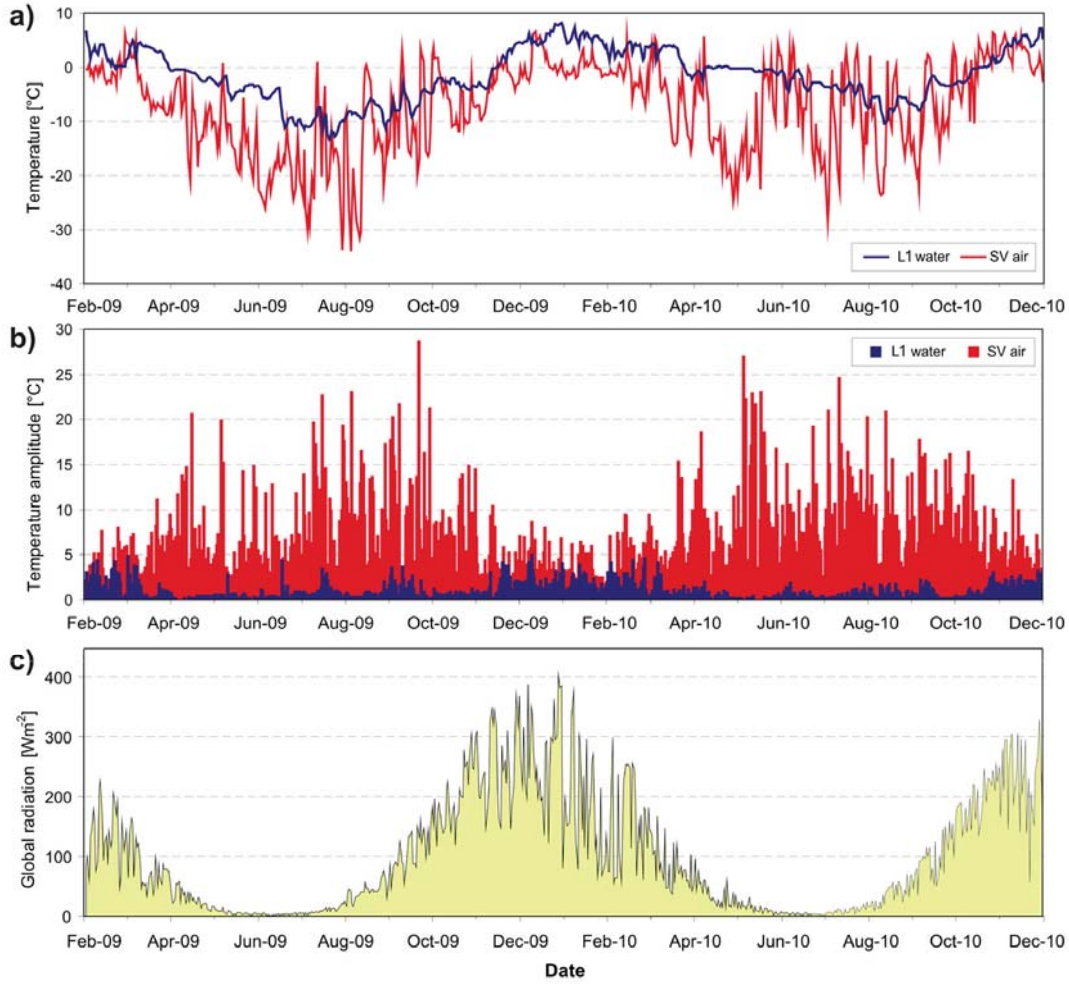
a)
Temperature [°C]
10
0
-10
-20
-30
-40
L1 water
SV air
Feb-09
Apr-09
Jun-09
Aug-09
Oct-09
Dec-09
Feb-10
Apr-10
Jun-10
Aug-10
Oct-10
Dec-10
b)
Temperature amplitude [°C]
30
25
20
15
10
5
0
L1 water
SV air
c)
Global radiation [Wm²]
400
300
200
100
0
Date

Fig. 3

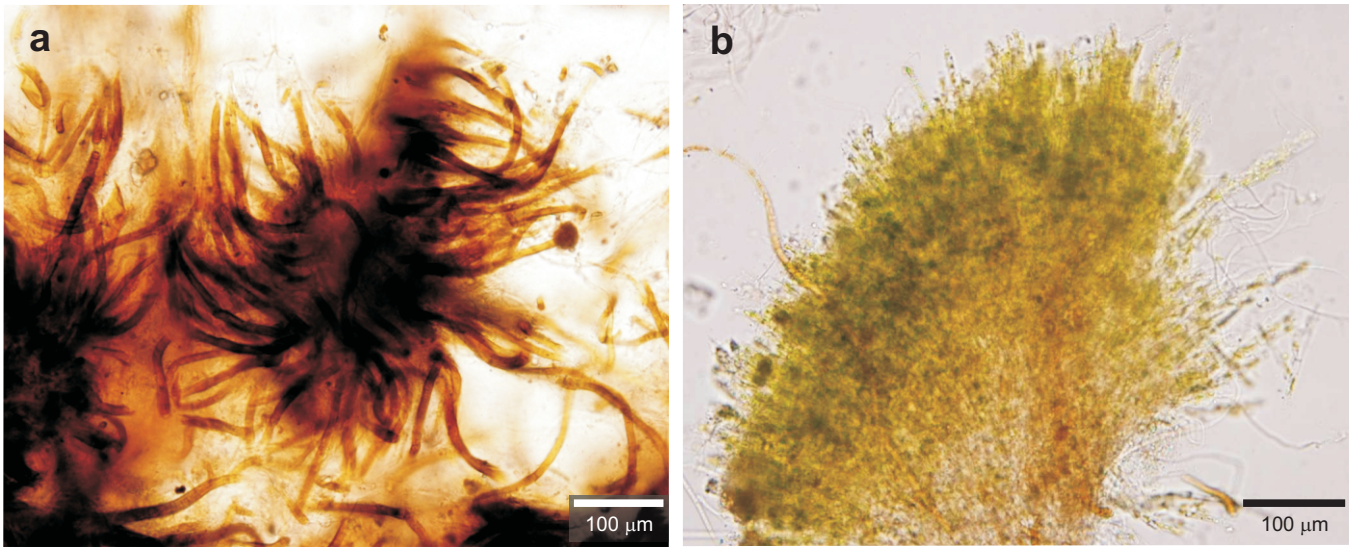

Fig. 4

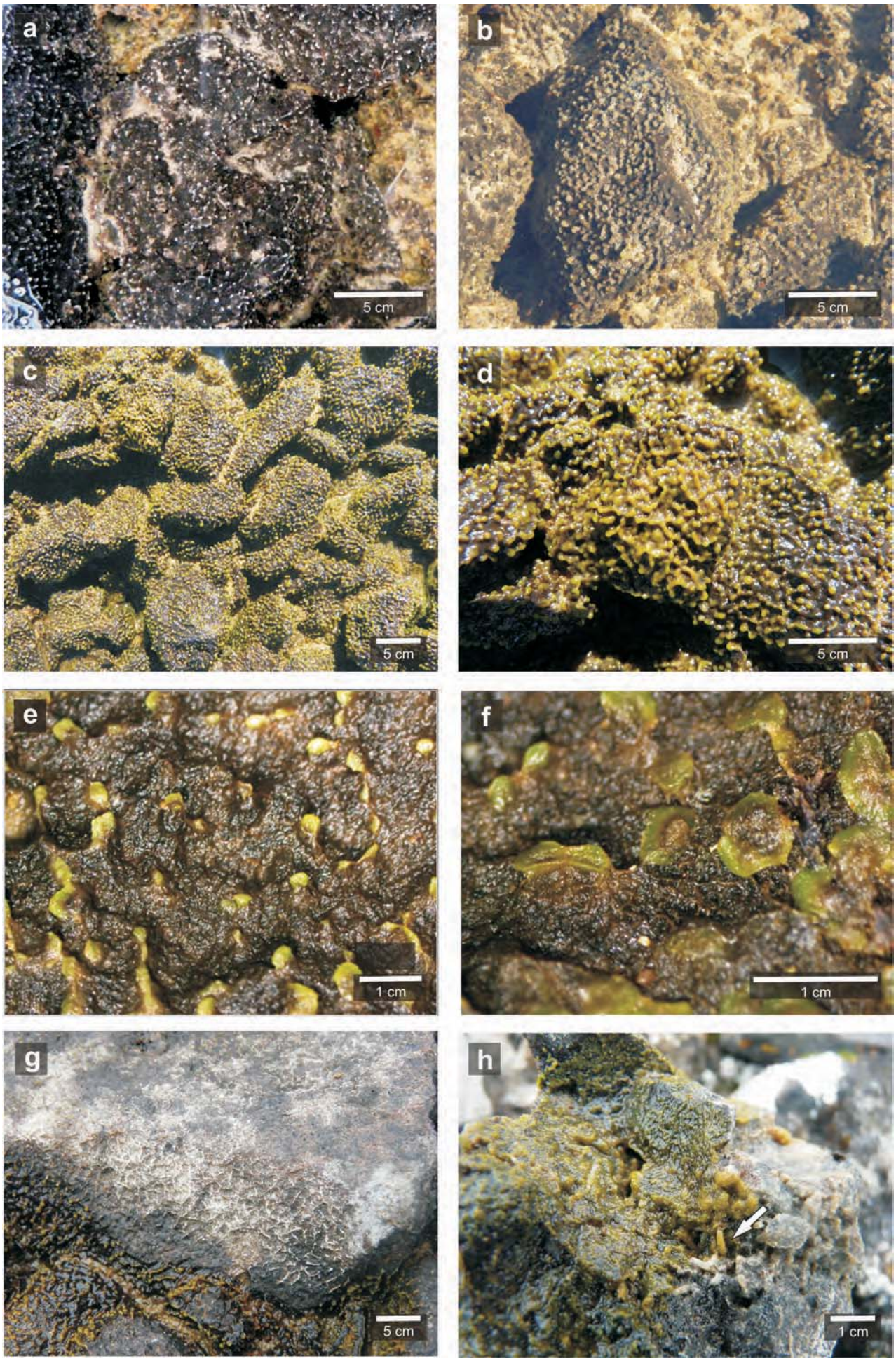

Fig. 5

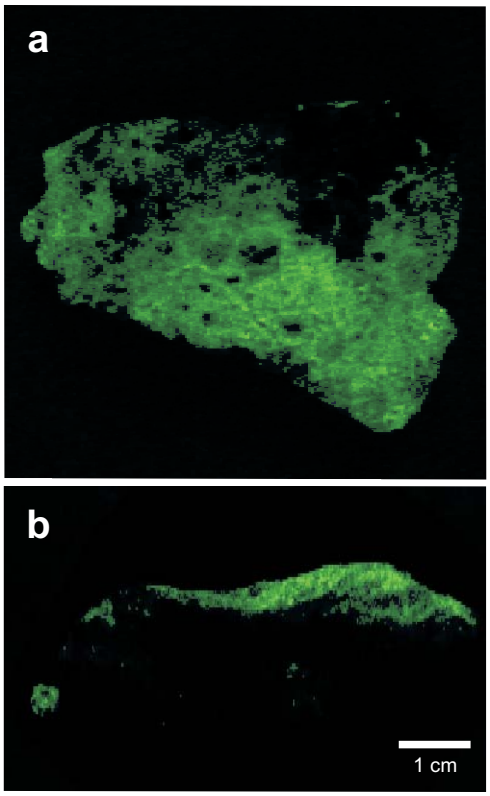

Fig. 6

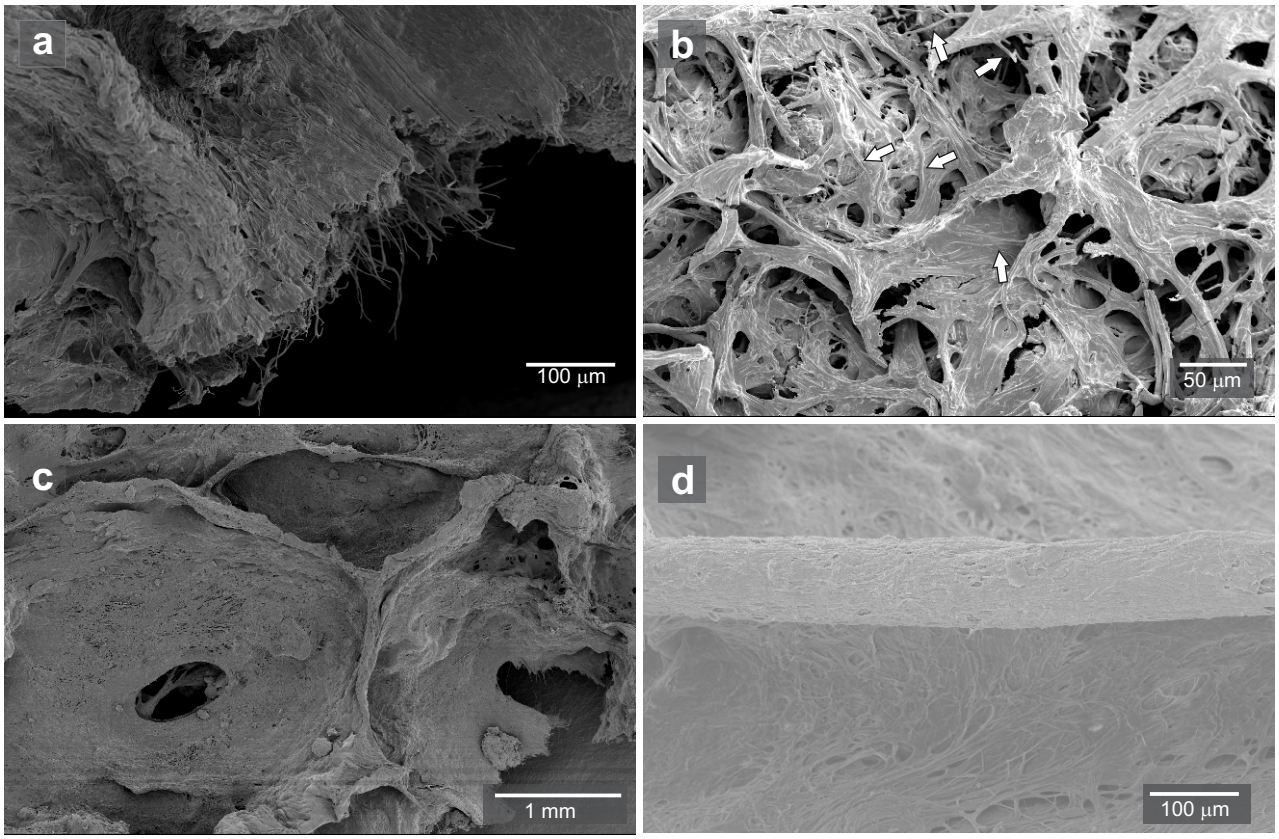

Fig. 7

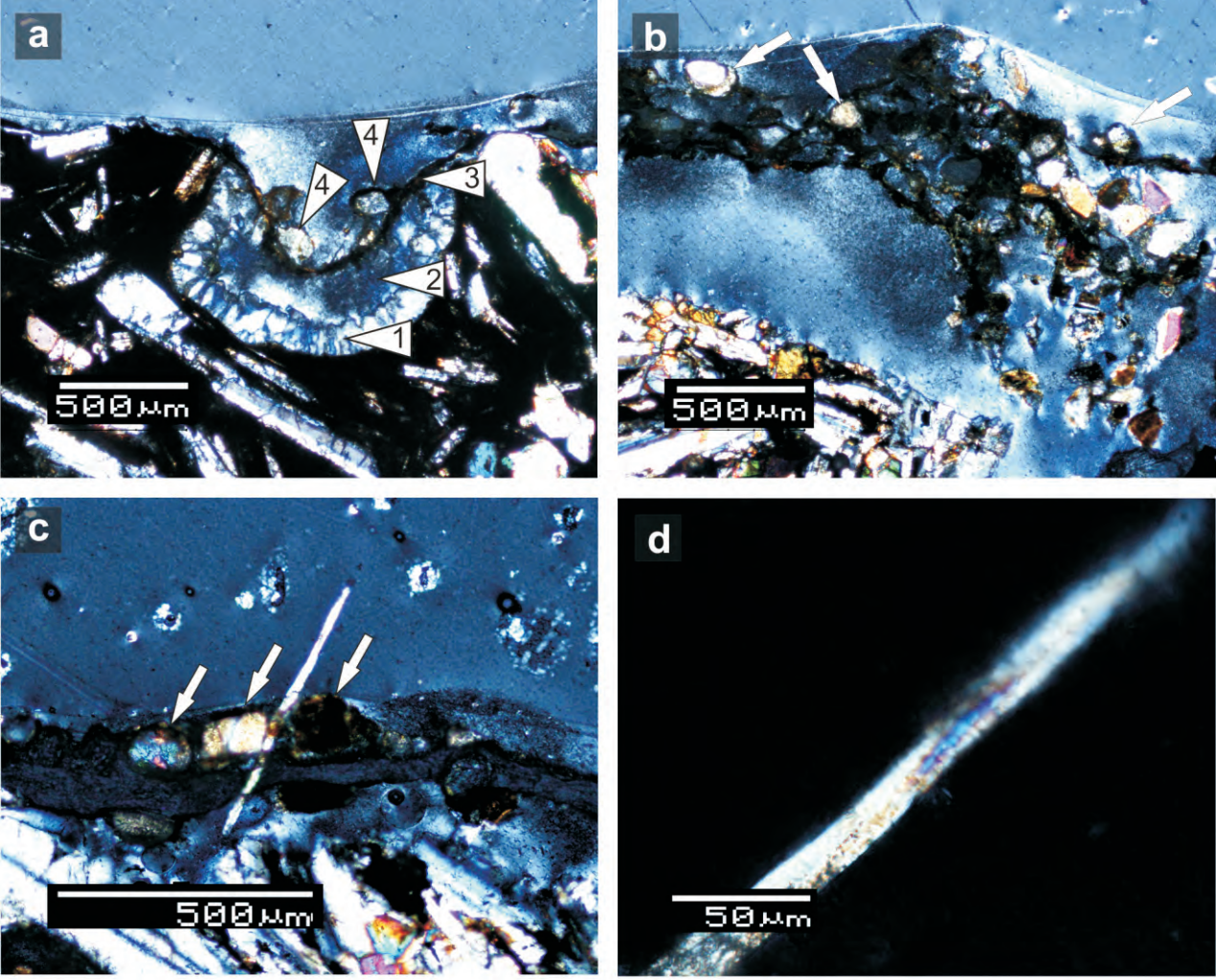

Fig. 8

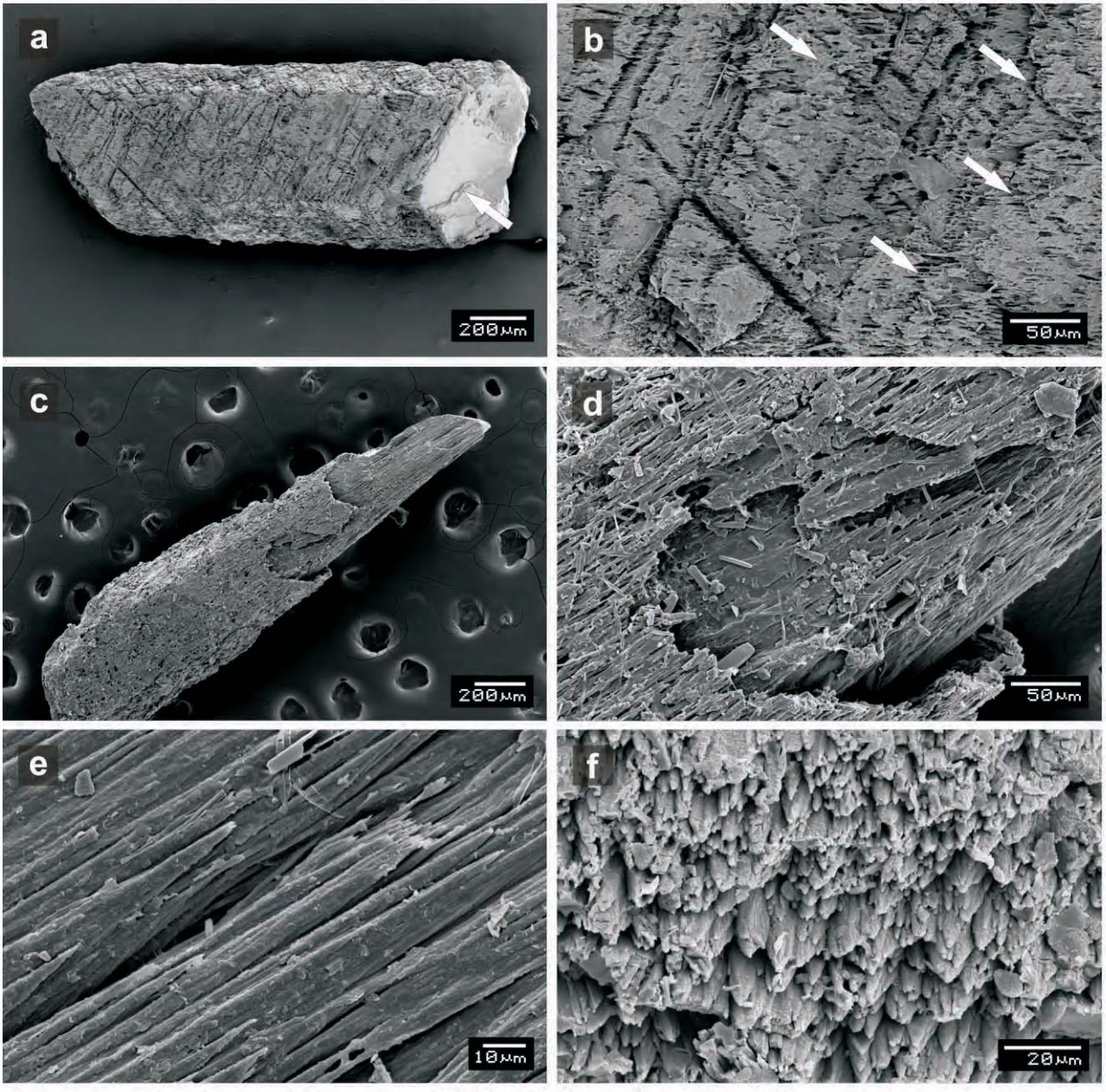

Fig. 9

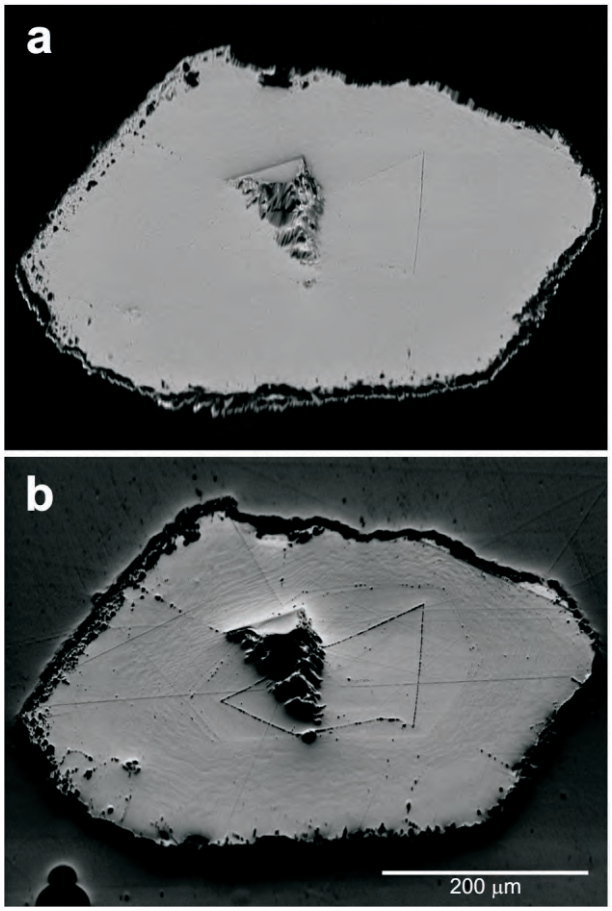

Fig. 10